

Simple Mechanical Equivalents of Stepping Rotary Dynamics in F_1 -ATPase

A.V. Zolotaryuk^{1,2}; V.N. Ermakov^{1,2}, P.L. Christiansen², B.Norden³, and Y. Zolotaryuk^{1,2}

¹Bogolyubov Institute for Theoretical Physics, 03143 Kyiv, Ukraine

²Section of Mathematical Physics, IMM, Technical University of Denmark, DK-2800 Lyngby, Denmark

³Department of Physical Chemistry, Chalmers University of Technology, S-412 96 Gøteborg, Sweden

(February 8, 2002)

Abstract

Two simple (rotator and one-particle) mechanistic models are suggested to describe simultaneously at a minimal level of sophistication two basic functions of F_1 -ATPase: a motor regime driven by ATP hydrolysis and its inverted function as ATP synthesis. This description is consistent with the so-called rotary binding-change mechanism, a milestone of functioning ATP synthase, and uses a stepping (driving) function associated with two sequences of time instants, at which hydrolysis and synthesis reactions occur. It is useful to analyse experimental data and numerical simulations indeed predict corresponding dynamic behavior.

PACS numbers: 05.60.-k, 05.40.-a, 87.10.+e

Recently, the modeling of molecular motors – enzymes which transduce chemical energy into directed mechanical motion – based on the idea of gaining useful work by rectification of zero-mean noise fluctuations has attracted considerable attention [1] and several models exploiting the so-called ratchet mechanism have been elaborated (see, e.g., Refs. [2–9], to

mention a few). In this context, ATP (adenosinetriphosphate) synthase shown schematically in Fig. 1, being a realistic molecular engine of great interest nowadays [10], should also be studied from the point of view of biological physics [11]. This machinery is composed of two rotary motors: a membrane-embedded unit F_0 and water-surrounded F_1 -ATPase (also called F_1) connected by a coiled-coil subunit. ATP synthase works as a reversible motor-pump machine: the proton flow through F_0 is believed to create a clockwise (when F_1 is viewed from the F_0 side) torque that turns F_1 , whereupon ATP molecules are sequentially synthesized at three catalytic sites, one on each F_1 subunit. Vice versa, ATP hydrolysis, which also occurs sequentially on F_1 's, but in the opposite direction, has been demonstrated to make F_1 rotate backwards, converting F_0 into a proton pump. In this case, F_1 is driven by sequential hinge-bending motions of F_1 's, like a crankshaft by the pistons in a car engine (for more details see Ref. [12]). In this paper, we focus on F_1 -ATPase and consider its operation in both hydrolysis (as a motor) and synthesis (as a synthesizer) directions, using in parallel two simple mechanistic analogs: a plane rotator and a particle subjected to a periodic potential. Our description is consistent with Boyer's binding-change mechanism [13,14], the recent findings of Cherepanov et al. and Junge et al. [15] on elasticity properties of the F_0 subunit, as well as with the experimental results of Yasuda et al. [16].

The structure of F_1 -ATPase and the mechanics of motions within it are too complex to allow a detailed description of all interactions and motions of its different parts, i.e., the three F_1 and one F_0 subunits [10,12,14,17-19]. Therefore, it would be useful to describe this very sophisticated three-dimensional system, using simple mechanical equivalents (springs, particles, etc.) and keeping the main features of rotary dynamics found in previous studies, such as the modeling of Oster and Wang [12] and others [10,15-19]. This approach, "from complexity to simplicity", is often used in biological physics. The typical example of such a modeling is the propagation of a nerve impulse on the giant axon of the squid, where insight in the dynamics of the original Hodgkin-Huxley equations [20] has been obtained by reduction to the minimal FitzHugh-Nagumo system [21].

Here the three-dimensional and four-body interaction in the F_1 subcomplex is suggested

to be effectively described as a coupling of a planar rotator of length R_0 centered in the middle of an equilateral triangle (see left panels of Figs. 2 and 3) with three equivalent catalytic sites (denote them by numbers 1, 2, and 3) at the vertices of the triangle. Obviously, this rotor-stator interaction, resulting in a crankshaft-like rotation of θ (and cooperative catalysis on θ 's), is a periodic function: $U(\theta + 2\pi) = U(\theta)$, where θ denotes the angular position of the rotator (positive if counter-clockwise). The mechanical equivalent of a driving torque on θ can be chosen as a stretched spring or an effective particle displaced from equilibrium in the periodic potential $U(\theta)$ as illustrated in the left and the right panels of Figs. 2 and 3, respectively. At each site $i = 1; 2; 3$, a spring K_i is attached connecting this site with the rotator. All the three springs are supposed to be identical, but only one spring is allowed to be switched on, while the other two are switched off, at a time. Then sequential switching the springs will result in a power stroke on θ . Without loss of generality, the rotor-stator potential (given in units of the hydrolysis energy $W \approx 80 \text{ pN} \cdot \text{nm}$) can be written as

$$U(\theta) = [r(\theta) - a]^2 / (1 - a)^2; \quad (1)$$

where $a = d/R_0$ is the length of each spring K_i being undistorted, $r(\theta) = \frac{q}{1 + (1 + a)^2 - 2(1 + a)\cos\theta}$ the instantaneous spring length, and $l = r(\theta = 2\pi/3)$.

Let us now describe how our spring system operates in both the hydrolysis and synthesis directions and how it can be coordinated with ATP hydrolysis/synthesis reactions at the catalytic sites of the subunits. According to Boyer's hypothesis [13] supported by the structural studies by Walker and coworkers [14], and recently by direct observation of Noji et al. [18], each site 1, 2, or 3 can be found at least in one of the three states: T (ATP binding), E (empty), and D (ADP binding), at a time. Structurally, they are arranged as T, E, and D counter-clockwise (see Figs. 1-3) and can be put on the θ axis at the lattice ("catalytic") sites with spacing $\theta = 2\pi/3$, as shown in the right panels of Figs. 2 and 3. The dimensionless periodic (with period 2π) potential $U(\theta)$ [not necessary of the form (1)] is supposed to be "rigidly tied" to this lattice, so that its minima are always found at sites with state T. We assume this potential to satisfy the normalization conditions: $U(T) = 0$

and $U(D) = 1$. The last constraint means that the potential energy of the effective particle in state D is equal to the free hydrolysis energy W .

Consider first the hydrolysis direction when F_1 operates as a motor (see Fig. 2). Let initially the subunit (rotor) be found at equilibrium, performing there thermal fluctuations. This state is represented by spring K_1 being undistorted and switched on state T , while the springs at the other sites (K_2 and K_3) are switched off. In the particle equivalent, this situation is represented in the right panel of Fig. 2 (a) by a particle fluctuating in the vicinity of one of them in a of the potential $U(\theta)$, i.e., in state T . When an ATP molecule settles into site 2 which is found at this time in state E , it appears bound there, resulting in ATP binding: $E \rightarrow T$. According to the rotary binding-change mechanism [13,14], this transition implies the two conformational changes at the next two sites: release of the inorganic phosphate (P) and the ADP (adenosinediphosphate) molecule from site 2 ($D \rightarrow E$), and hydrolysis of the ATP molecule located at site 3 ($T \rightarrow D$). After these state transitions have occurred, spring K_1 is switched off, while spring K_2 is switched on, causing the power stroke on the rotor as demonstrated by Fig. 2 (b). Therefore the rotor is driven forward before it reaches a new equilibrium state, stepping forward by $2\pi/3$. Correspondingly, as shown in the right panel, the potential $U(\theta)$ steps forward (to the right) by $2\pi/3$, so that the particle appears to be lifted uphill at the level $U = 1$, thereafter sliding down and finally dwelling in the next potential minimum before the next sequence of conformational changes takes place. However, if occasionally two sequential conformational transitions occur very close in time resulting in two almost simultaneous potential steps forward, the particle appears on the positive slope of the potential $U(\theta)$, sliding thereafter down backwards. When the time between two sequential transitions is still short, but long enough for the particle to make a descent close to equilibrium, the double potential step forward will result in the double sliding down on the negative slope. Indeed, both such occasional steps of loaded by an actin filament were observed in experiments [16,18,19]. We denote the sequence of time instants when hydrolysis events occur by $t_1^+ g_{i=1}^1$ and call it a "hydrolysis sequence".

Consider now the case, when an external torque (e.g., from the side of F_0) is applied to

the subunit clockwise, as shown in the left panel of Fig. 3 (a). According to Cherepanov et al. and Junge et al. [15], the external energy of torsion is stored as an elastic strain energy of . When the rotor turns clockwise totally by $2\pi/3$, the torsional energy is liberated for the synthesis of one ATP molecule at the site being in state D. Then spring K_1 is switched off, while spring K_3 is on, bringing the system to the zero-energy level ($U = 0$). Equivalently, the particle "drops down" to equilibrium state T [see Fig. 3 (b)]. These mechanical equivalents are again in accordance with Boyer [13] for ATP synthesis, when the conformational change $D \rightarrow T$ implies the transitions at the other two sites: $T \rightarrow E$ and $E \rightarrow D$. We denote the sequence of time instants when synthesis events occur by $\{t_j\}_{j=1}^1$ and call it a "synthesis sequence".

Summarizing, one can present the diagram shown in Fig. 4, which describes the elastic strain energy of the torsional rotor-stator interaction as a function of θ , combining both the hydrolysis and synthesis directions. A row shows the rotational direction under hydrolysis ($\dot{\theta} > 0$, motor regime) and synthesis ($\dot{\theta} < 0$, synthesizer regime).

In experiments [16,18,19], the subunit was loaded by an actin filament rotating in a viscous solution. Therefore, we approach the overdamped limit and the equation of motion for the rotator driven by a periodic potential $U(\theta)$ fluctuating stepwise forward and backwards by $2\pi/3$ (due to hydrolysis power strokes and an external load torque T_1) reads

$$-\gamma \dot{\theta} = W @ U [\theta - 2\pi S(t)/3] - T_1(\theta; t) + \xi(t); \quad (2)$$

where γ is a viscous friction coefficient, $U(\theta)$ is normalized by $U(2\pi n) = 0$ and $U[2\pi(n+1/3)] = 1$, $n = 0; 1; \dots$, and $\xi(t)$ is the Brownian torque with the auto-correlation function $\langle \xi(t) \xi(t^0) \rangle = 2 k_B T \delta(t - t^0)$, where k_B denotes Boltzmann's constant and T is the absolute temperature. The stepping (driving) function

$$S(t) = \sum_{i=1}^1 \chi_i(t - t_i^+) - \sum_{j=1}^1 \chi_j(t - t_j); \quad (3)$$

where $\chi(t) = 0$ for $t < 0$ and $\chi(t) = 1$ for $t \geq 0$, is defined through the two time sequences $\{t_i^+\}_{i=1}^1$ and $\{t_j\}_{j=1}^1$ indicating the time instants when hydrolysis and synthesis reactions occur, respectively.

The hydrolysis sequence t_{i+1}^+ is a random process determined by ATP concentration $[ATP]$. We define it through two characteristic duration times t_D and t_T by the recurrence relation

$$t_{i+1}^+ = t_i^+ + t_D + 2\alpha_{i+1} t_T; i = 1; 2; \dots; \quad (4)$$

where each $\alpha_i \in [0; 1]$ is a random value with uniform distribution (since ATP concentration is supposed to be constant in the solution). The interval t_T is large for low $[ATP]$, but tends to zero as $[ATP]$ is sufficiently high. Therefore one can assume that $t_T = A_T/[ATP]$ with some constant $A_T > 0$. The interval t_D triggers the hydrolysis reactions by release of P and ADP on the next site of the stator. In the limit of low concentration of nucleotides (ATP and ADP), this interval is short, whereas for high concentration, the release of the hydrolysis products is impeded and therefore some saturation for t_D takes place. As a result, one can assume that $t_D = t_{st}[ATP] = (C_D + [ATP])$ with some constant $C_D > 0$ and t_{st} being the duration time of one step. At zero temperature, it follows from the overdamped dynamics governed by Eq. (2) that $t_{st} \rightarrow 1$ (an overdamped particle approaches a potential minimum after an infinitely long time). However, at nonzero temperature, the time for one step becomes finite, because in the vicinity of equilibrium, the particle is "captured" by thermal fluctuations. Thus, in the limit $\alpha \rightarrow 0$, the potential (1) is reduced to the simple form $U = 2(1 - \cos \theta) = 3$, admitting an explicit solution of Eq. (2) for each step if $\langle \theta \rangle = 0$. Since the average amplitude of thermal fluctuations is $\sqrt{\frac{q}{3D}} = \sqrt{2}$, one finds that $t_{st} = (3t_0 = 2) \ln \frac{p}{3\cot \frac{q}{3D}} = 8$, where $t_0 = \frac{\eta}{W}$ is the time unit and $D = \frac{k_B T}{\eta}$ the dimensionless strength of white noise in Eq. (2). Since, at room temperature $k_B T \approx 4$ pN nm, we thus have $D \approx 0.05$, so that t_{st} can be estimated for each viscous load η .

Averaging Eq. (4), one finds that $\langle t_{i+1}^+ - t_i^+ \rangle = t_D + t_T$ and therefore the rotational rate of (number of revolutions per second) is $V = [3(t_D + t_T)]^{-1}$. Inserting here the dependences of $t_{D,T}$ on $[ATP]$ given above, one finds

$$V = \frac{V_{max}[ATP]}{K_M + [ATP] + (C_D + [ATP])}; \quad (5)$$

where $V_{max} = (3 t_{st})^{-1} = (t_D)^{-1}$ is a maximal average velocity (as $[ATP] \rightarrow 1$) and the constant $K_M = A_T = t_{st}$ can be identified as the Michaelis constant, because Eq. (5) is reduced to the Michaelis-Menten law in the limit $C_D \rightarrow 0$. According to Yasuda et al. [16], $K_M = 0.8 \text{ M}$ and $V_{max} = 4 \text{ s}^{-1}$, and for these values the dependence (5) is shown in Fig. 5 (including the experimental data), with monotonic behavior for $C_D > K_M$. Similarly [16], one can assume that the one-step duration depends on the length of the filament L as $t_{st} = g_0 + g_1 L^3$, and substituting this expression into Eq. (5), one finds for small C_D the dependence $V(L) = \frac{1}{3} (A_T = [ATP] + g_0 + g_1 L^3)^{-1}$ plotted in Fig. 6, where the constants A_T and $g_{0,1}$ are fitted to the experiments [16].

As described above, for a given random hydrolysis sequence (4), each synthesis instant t_j is defined as the time when the rotor, being at some time in state T , rotates backwards by $2\pi/3$. Direct simulations of the dimensionless ($t = t_0$) equation (2) with the potential (1) are presented in Fig. 7. Here the intervals $t_{D,T} = t_{D,T} - t_0$ in the sequence (4) are given through the constants C_D and K_M , as well as the parameter $t_{st} = t_{st} - t_0 = W/3 = V_{max}$ to be evaluated from experiments. Thus, using that $(L = 1 \text{ nm})^{-1} = 1 \text{ pN nm}$ and $V_{max} = 4 \text{ s}^{-1}$ [16], one finds $t_{st} = 6.75$: In the case without load (curves 1 and 2), the average velocity $\langle \dot{\theta} \rangle = V = W$ is in good agreement with the direct observations (see Fig. 3 of Ref. [16]) and the law plotted in Fig. 5 at $C_D = K_M$, where the two velocities shown with dotted lines 1 and 2 correspond to curves 1 and 2 in Fig. 7, respectively. Note that the constant C_D in Eq. (5) implicitly describes the main feature of trajectories at low $[ATP]$ (see curve 2): on average the number of multi-steps exceeds that of steps backwards, as observed experimentally [18,16]. Next, when a load torque $T_1 > 0$ is applied, the rotational rate decreases with increase of this torque, as illustrated by curve 3 in Fig. 7. Moreover, when the load exceeds some threshold value, the motor operates in inverse, as shown by curves 4 and 5. Similarly to Lattanzi and Maritan [8], the law (5) can be modified by subtracting a positive constant that controls the direction of rotation if $T_1 > 0$.

Thus, we have developed two (rotator and one-particle) physical models of archetypal

simplicity, which are consistent with the rotary binding-change mechanism [13,14] and the elasticity properties of the subunit [15]. The cooperative rotational catalysis at the three subunits is described through two time sequences, each for switching hydrolysis and synthesis reactions, by adjusting the statistics of switching to satisfy the recent experimental results [18,16]. The models described in this paper are generic and simple; they do not depend on details of the periodic potential $U(\theta)$. In the hydrolysis (motor) direction, the subunit works in a "passive" regime; only all the subunits are coordinated in the cooperative rotational catalysis. In the reversible (synthesis) direction, it is "active", causing the corresponding (again cooperative, but in the inverse sequence) conformational changes after its strain energy of torsion reaches the free ATP hydrolysis energy. These important features are consistent with both Boyer's binding-change mechanism [13,14] and the findings of Cherepanov et al. and Junge et al. [15]. The dependences of the model parameters on ATP concentration are general and physically motivated. In the framework of our description, the load torque $T_L(\theta; t)$ generated by the F_0 part can further be involved explicitly resulting in a general motor/pump model of ATP synthase.

We also conclude that the puzzle, how does the binding-change mechanism work, may be essential not only for understanding the chemistry (dissipative catalysis) of creation of ATP, one of the most important processes in life, but also constitute a key physical problem behind the function of molecular motors, such as design of man-made molecular devices.

We acknowledge partial financial support from the European Union under the INTAS Grant No. 97-0368 and the LO CNET Project No. HPRN-CT-1999-00163. We thank A.C. Scott for stimulating and helpful discussions.

REFERENCES

- [1] R.D. Astumian, *Science* 276, 917 (1997); F. Julicher, A. Ajdari, and J. Prost, *Rev. Mod. Phys.* 69, 1269 (1997); P. Reimann, *Phys. Reports* 361, 57 (2002).
- [2] R.D. Astumian and M. Bier, *Phys. Lett. Lett.* 72, 1766 (1994).
- [3] J. Prost et al., *Phys. Lett. Lett.* 72, 2652 (1994).
- [4] I. Derenyi and T. Vicsek, *Proc. Natl. Acad. Sci. USA* 93, 6775 (1996); G.N. Stratopoulos, T.E. Djalynas, and G.P. Tsironis, *Phys. Lett. A* 252, 151 (1999).
- [5] F. Marchesoni, *Phys. Lett. A* 237, 126 (1998); M. Borromeo and F. Marchesoni, *Phys. Lett. A* 249, 199 (1998).
- [6] S. Cilla and L.M. Floria, *Physica D* 113, 157 (1998); S. Cilla, F. Fab, and L.M. Floria, *Phys. Rev. E* 63, 031110 (2001).
- [7] M. Porto et al., *Phys. Rev. Lett.* 85, 491 (2000).
- [8] G. Lattanzi and A. Maritan, *Phys. Rev. Lett.* 86, 1134 (2001).
- [9] C. Bustamante, D. Keller, and G. Oster, *Acc. Chem. Res.* 34, 412 (2001).
- [10] For recent reviews on ATP synthase see special issue 2-3, *Biochim. Biophys. Acta* 1458 (2000).
- [11] H. Frauenfelder et al., *Rev. Mod. Phys.* 71, S419 (1999).
- [12] G. Oster and H. Wang, *Biochim. Biophys. Acta* 1458, 482 (2000); H. Wang and G. Oster, *Nature (London)* 396, 279 (1998).
- [13] P.D. Boyer, *Biochim. Biophys. Acta* 1140, 215 (1993).
- [14] J.P. Abrahams et al., *Nature (London)* 370, 621 (1994).
- [15] D.A. Cherepanov et al., *FEBS Lett.* 449, 1 (1999); W. Junge et al., *ibid.* 504, 152 (2001).

- [16] R. Yasuda et al, Cell 93, 1117 (1998).
- [17] D. S. Sabbert, S. Engelbrecht, and W. Junge, Proc. Natl. Acad. Sci. USA 94, 4401 (1997).
- [18] H. Noji et al, Nature (London) 386, 299 (1997).
- [19] K. Kinoshita et al, Cell 93, 21 (1998).
- [20] A. L. Hodgkin and A. F. Huxley, J. Physiol. 117, 500 (1952).
- [21] R. FitzHugh, Biophys. J. 1, 445 (1961); J. Nagumo et al, Proc. IRE 50, 2061 (1962).

FIGURE CAPTIONS

FIG . 1. Schematics of ATP synthase adapted from Ref. [19]. An asymmetric shaft rotates relatively to the hexamer formed by c and three a subunits arranged alternatively. The other subunits, which constitute F_0 including the "anchor" part are not shown. The positive direction of rotation and the directions of proton flow and rotational catalysis (sequential synthesis/hydrolysis reactions in the hexamer) are shown by the arrows.

FIG . 2. Spring (left panels) and particle (right panels) equivalents of the rotor-stator system evolving in hydrolysis direction. (a) Rotor (left) and particle (right) are found in equilibrium (in state T). (b) Power stroke caused by stretched spring K_2 will rotate counter-clockwise (left). Sliding the particle down on the negative slope of periodic potential $U(\theta)$, after it has moved forward by $2\pi/3$ (right).

FIG . 3. Spring (left panels) and particle (right panels) equivalents of the rotor-stator system evolving in synthesis direction. (a) External torque drives the rotator clockwise and elastic strain energy of the system is stored in spring K_1 (left). Lifting particle uphill in potential $U(\theta)$ (right). (b) Release of elastic strain energy after synthesis takes place (left). After the particle energy has reached the value $U = 1$, potential $U(\theta)$ steps backwards by $2\pi/3$, allowing the particle to "drop downhill" to zero energy level (right).

FIG . 4. Strain energy of the rotor-stator system against angular position θ in hydrolysis ($\Delta\mu > 0$) and synthesis ($\Delta\mu < 0$).

FIG . 5. Rotational rate of ω against ATP concentration calculated for three values of C_D , using Eq. (5). Experimental results [16] shown by circles are given for comparison.

FIG . 6. Rotational rate of ω against the length of actin filament: experimental results (circles, squares, and triangles) and dependences $V(L)$ calculated for three values of ATP concentration.

FIG . 7. Typical trajectories for different regimes of F_1 . Curves 1 and 2 demonstrate pure motor regime (without load) for high (curve 1; $C_D = 6.75$ and $\Delta\mu_T = 0$) and low (curve 2; $C_D = 2$, $\Delta\mu_T = 10$, $[ATP] = 0.4$ M, and $C_D = K_M = 0.8$ M) ATP concentration. The

other trajectories illustrate mixed motor/synthesizer regimes for different constant loads: below threshold (curve 3; $\gamma_D = 1.7$, $\gamma_T = 20$, and $T_l = 20$ pN nm), nearby threshold (curve 4; $\gamma_D = 6.75$, $\gamma_T = 0$, and $T_l = T_{th} \approx 38.4$ pN nm), and above threshold (curve 5; $\gamma_D = 6.75$, $\gamma_T = 0$, and $T_l = 0.48$ pN nm).

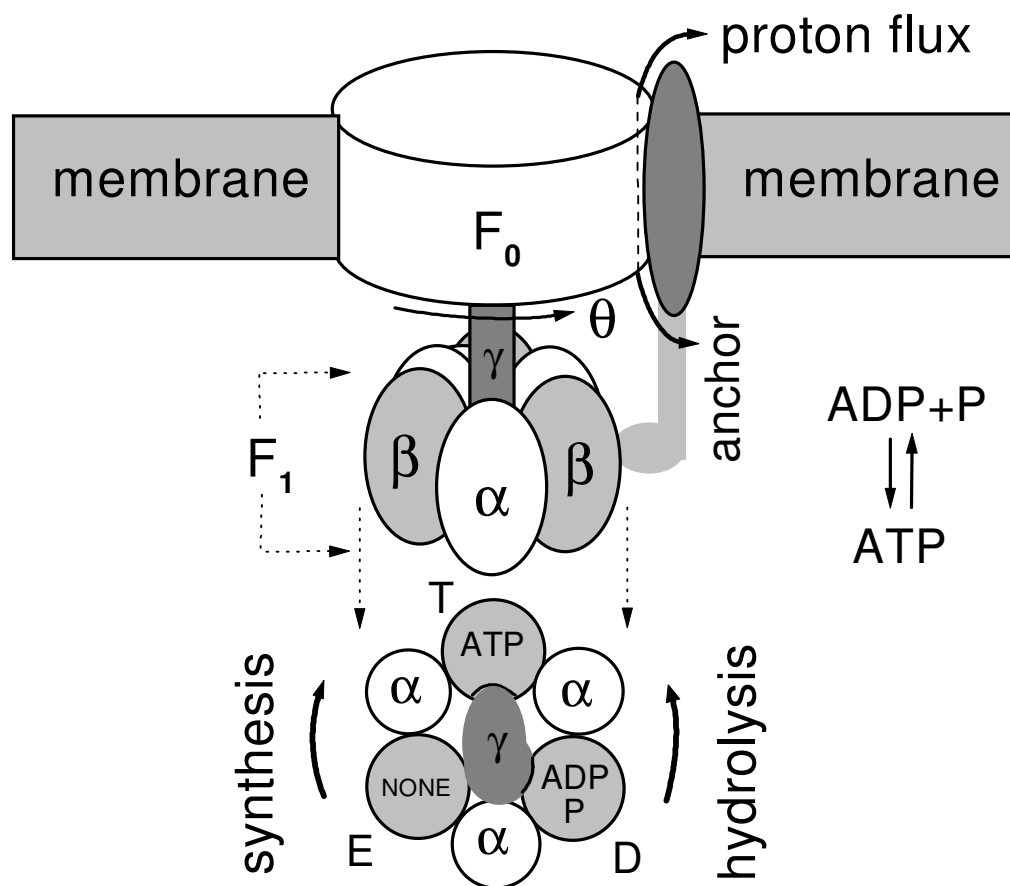


FIG.1. "Rotary Motion in F₁-ATPase: ...",
by A.V. Zolotaryuk et al.

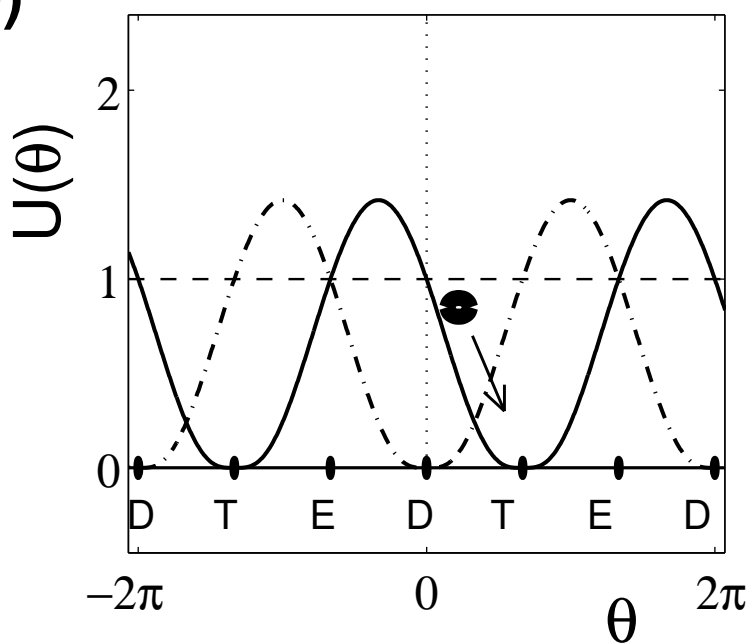
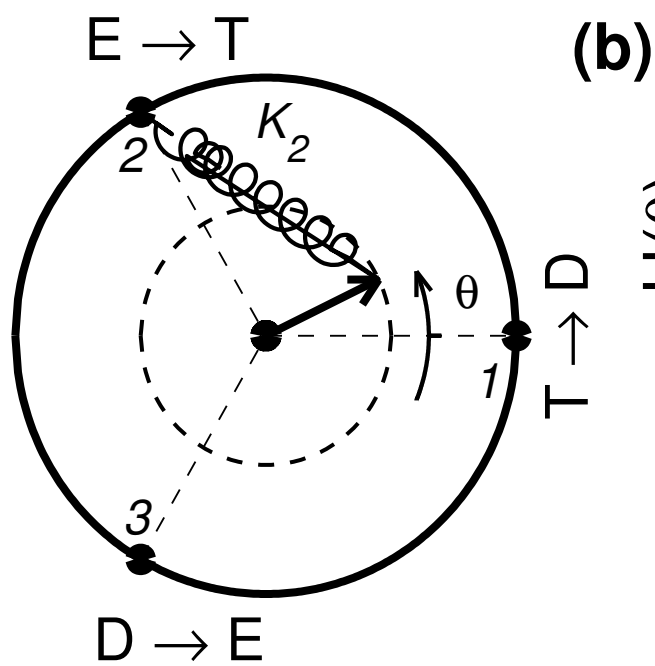
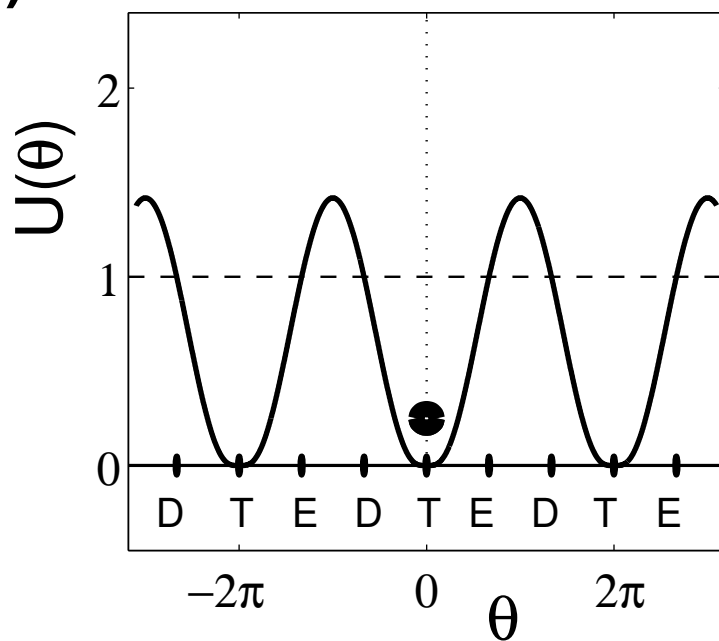
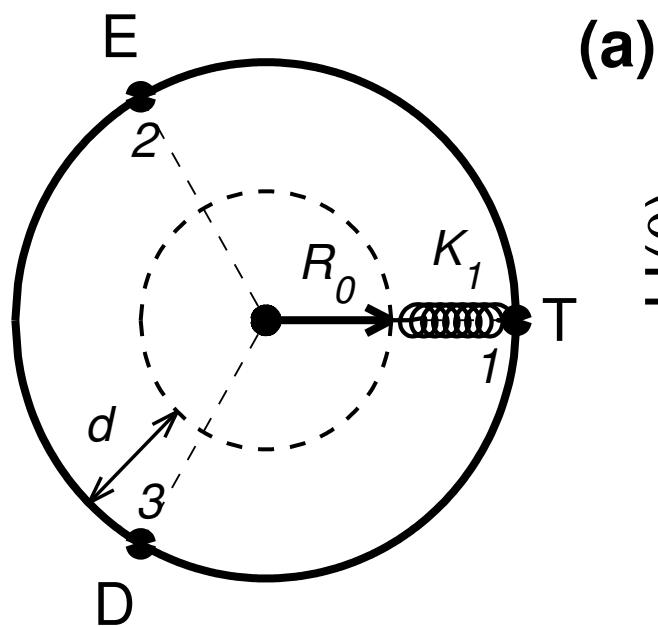


Fig. 2. "Rotary motion in F_1 -ATPase:...", by A. V. Zolotaryuk *et al.*

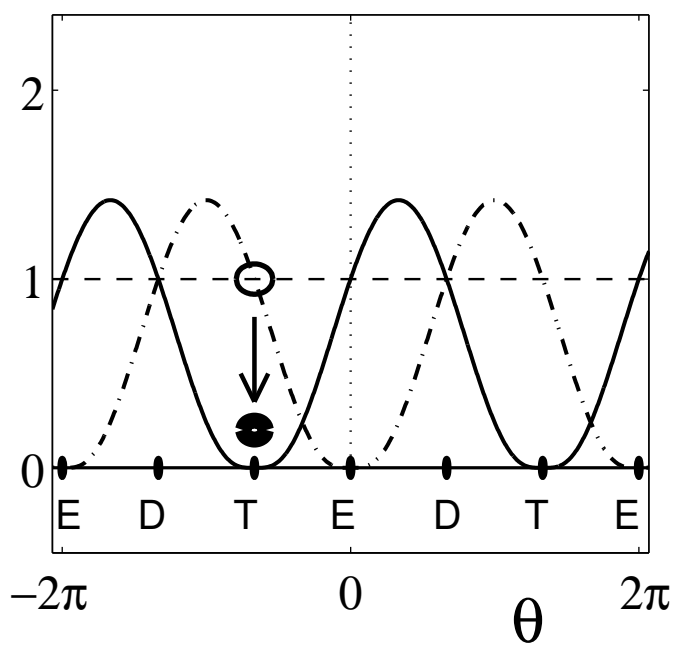
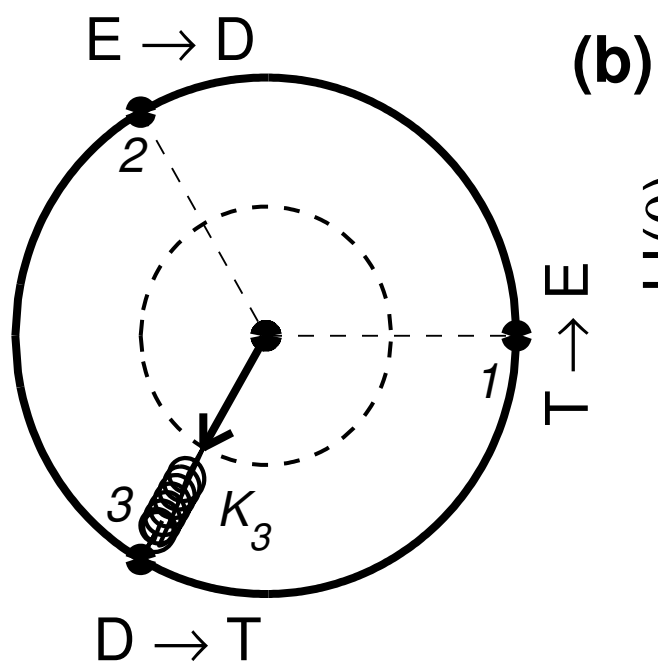
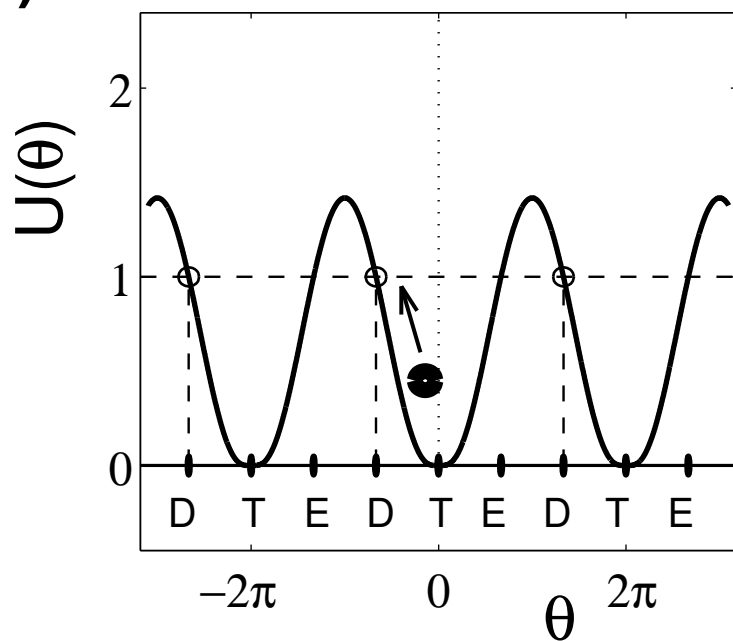
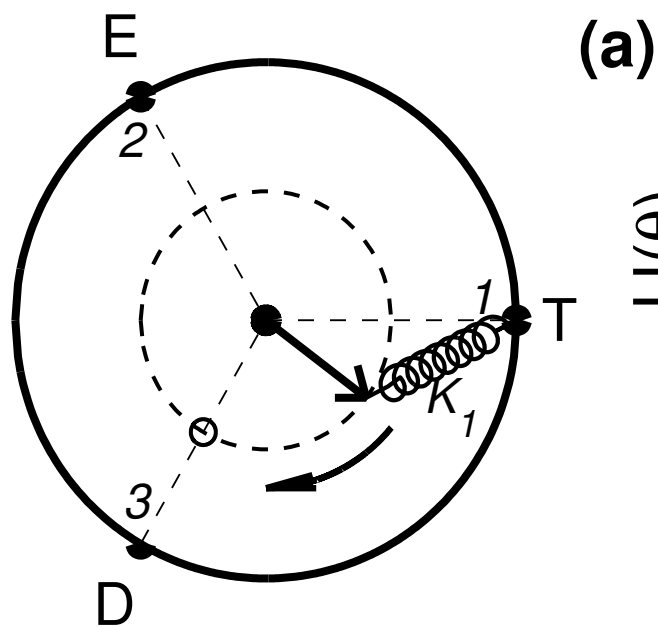


Fig. 3. "Rotary motion in F_1 -ATPase:...", by A. V. Zolotaryuk *et al.*

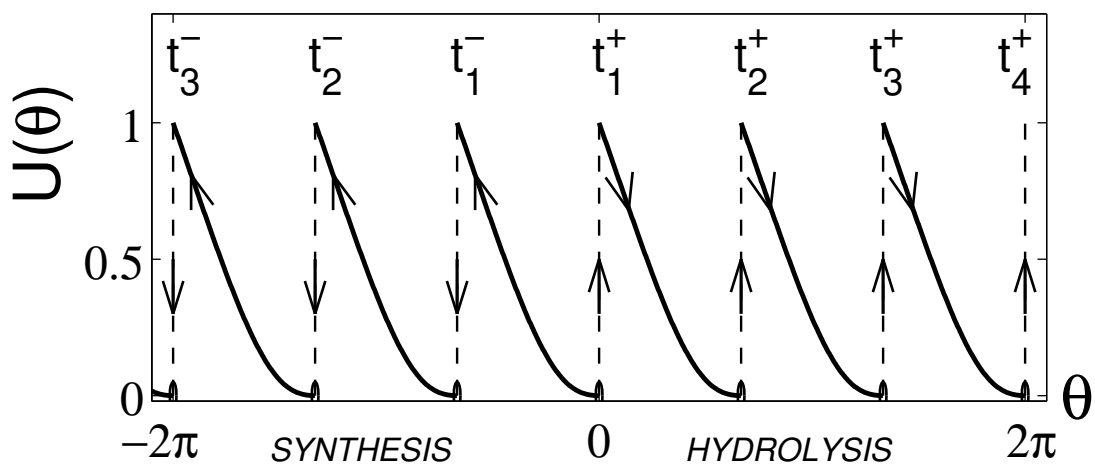


Fig. 4. "Rotary motion in F_1 -ATPase:...", by A. V. Zolotaryuk *et al.*

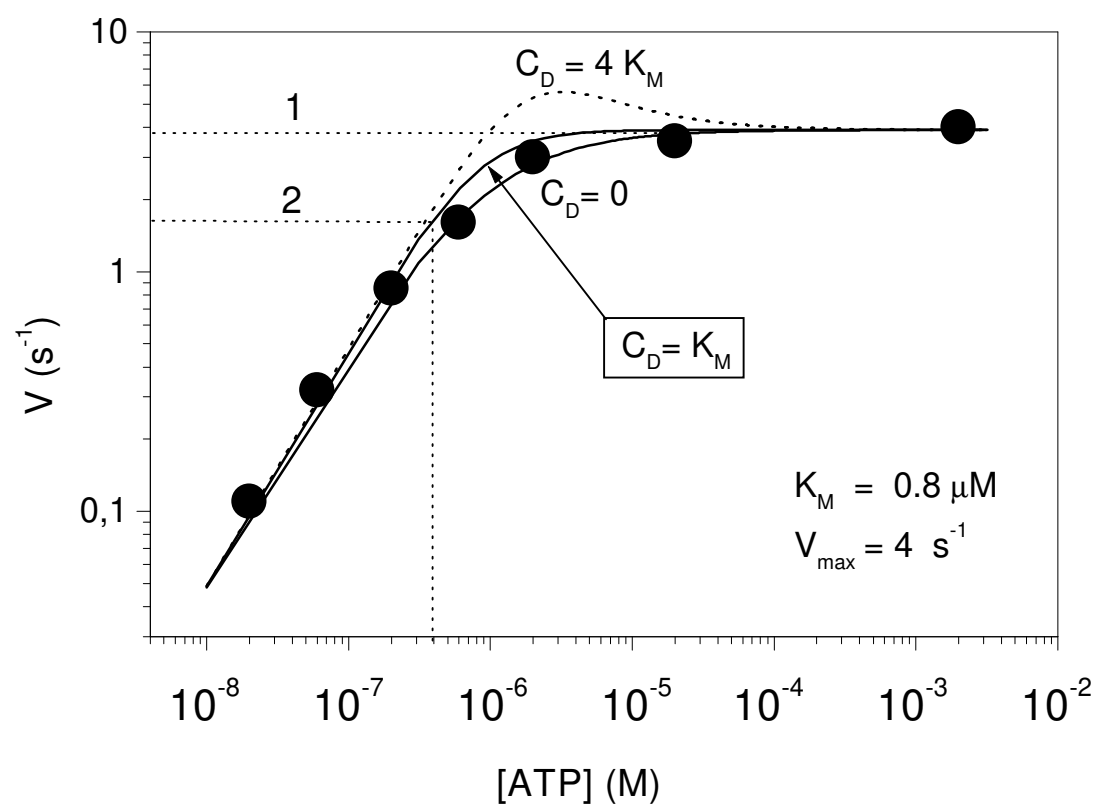


FIG.5. "Rotary Motion in F_1 -ATPase: ...",
by A.V. Zolotaryuk et al.

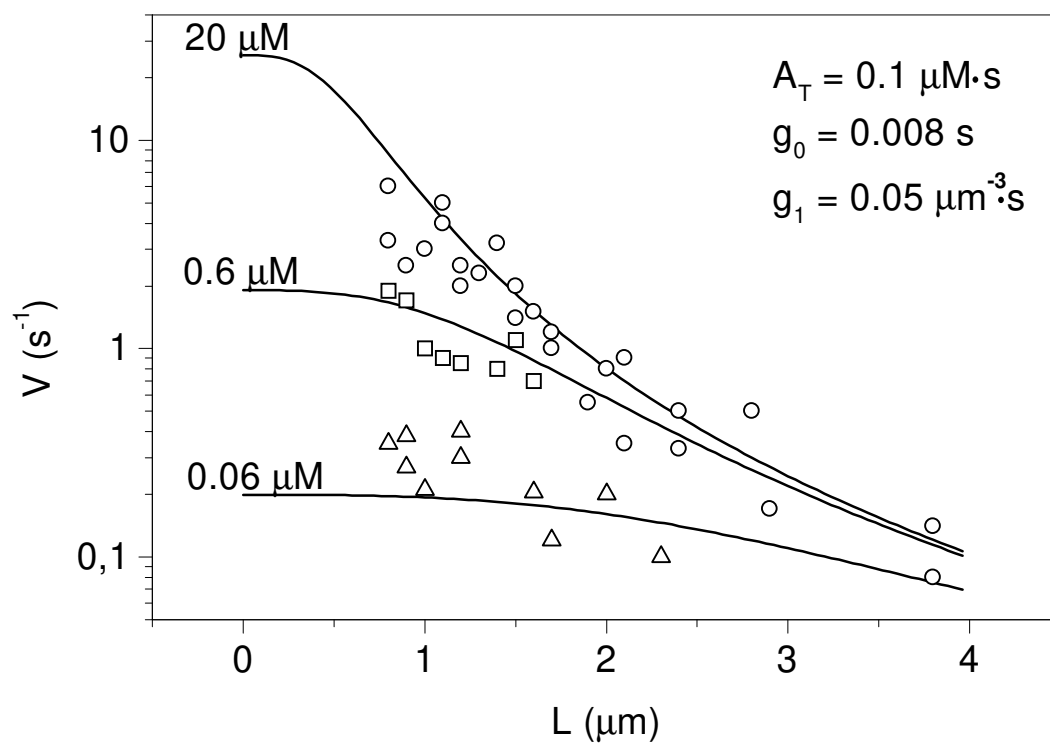


FIG.6. "Rotary Motion in F_1 -ATPase: ...",
 by A.V. Zolotaryuk et al.

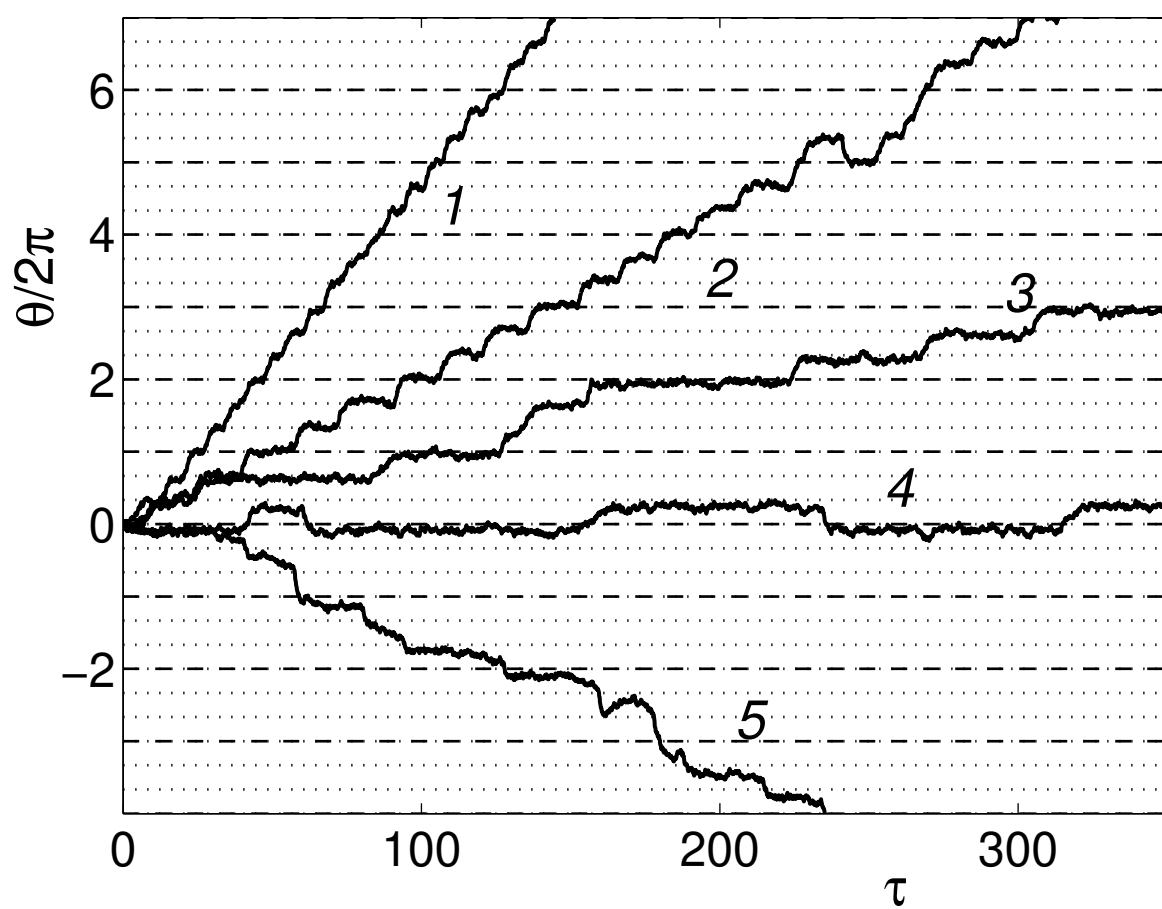


Fig. 7. "Rotary motion in F_1 -ATPase:...", by A. V. Zolotaryuk *et al.*